

Study of  $J/\psi \rightarrow \omega p \bar{p}$  at BESIII

1  
2 M. Ablikim<sup>1</sup>, M. N. Achasov<sup>6</sup>, O. Albayrak<sup>3</sup>, D. J. Ambrose<sup>39</sup>, F. F. An<sup>1</sup>, Q. An<sup>40</sup>, J. Z. Bai<sup>1</sup>, R. Baldini Ferroli<sup>17A</sup>,  
3 Y. Ban<sup>26</sup>, J. Becker<sup>2</sup>, J. V. Bennett<sup>16</sup>, M. Bertani<sup>17A</sup>, J. M. Bian<sup>38</sup>, E. Boger<sup>19,a</sup>, O. Bondarenko<sup>20</sup>, I. Boyko<sup>19</sup>, R. A. Briere<sup>3</sup>,  
4 V. Bytev<sup>19</sup>, H. Cai<sup>44</sup>, X. Cai<sup>1</sup>, O. Cakir<sup>34A</sup>, A. Calcaterra<sup>17A</sup>, G. F. Cao<sup>1</sup>, S. A. Cetin<sup>34B</sup>, J. F. Chang<sup>1</sup>, G. Chelkov<sup>19,a</sup>,  
5 G. Chen<sup>1</sup>, H. S. Chen<sup>1</sup>, J. C. Chen<sup>1</sup>, M. L. Chen<sup>1</sup>, S. J. Chen<sup>24</sup>, X. Chen<sup>26</sup>, Y. Chen<sup>1</sup>, Y. B. Chen<sup>1</sup>, H. P. Cheng<sup>14</sup>,  
6 Y. P. Chu<sup>1</sup>, D. Cronin-Hennessy<sup>38</sup>, H. L. Dai<sup>1</sup>, J. P. Dai<sup>1</sup>, D. Dedovich<sup>19</sup>, Z. Y. Deng<sup>1</sup>, A. Denig<sup>18</sup>, I. Denysenko<sup>19,b</sup>,  
7 M. Destefanis<sup>43A,43C</sup>, W. M. Ding<sup>28</sup>, Y. Ding<sup>22</sup>, L. Y. Dong<sup>1</sup>, M. Y. Dong<sup>1</sup>, S. X. Du<sup>46</sup>, J. Fang<sup>1</sup>, S. S. Fang<sup>1</sup>, L. Fava<sup>43B,43C</sup>,  
8 C. Q. Feng<sup>40</sup>, P. Friedel<sup>2</sup>, C. D. Fu<sup>1</sup>, J. L. Fu<sup>24</sup>, O. Fuks<sup>19,a</sup>, Y. Gao<sup>33</sup>, C. Geng<sup>40</sup>, K. Goetzen<sup>7</sup>, W. X. Gong<sup>1</sup>, W. Gradl<sup>18</sup>,  
9 M. Greco<sup>43A,43C</sup>, M. H. Gu<sup>1</sup>, Y. T. Gu<sup>9</sup>, Y. H. Guan<sup>36</sup>, A. Q. Guo<sup>25</sup>, L. B. Guo<sup>23</sup>, T. Guo<sup>23</sup>, Y. P. Guo<sup>25</sup>, Y. L. Han<sup>1</sup>,  
10 F. A. Harris<sup>37</sup>, K. L. He<sup>1</sup>, M. He<sup>1</sup>, Z. Y. He<sup>25</sup>, T. Held<sup>2</sup>, Y. K. Heng<sup>1</sup>, Z. L. Hou<sup>1</sup>, C. Hu<sup>23</sup>, H. M. Hu<sup>1</sup>, J. F. Hu<sup>35</sup>, T. Hu<sup>1</sup>,  
11 G. M. Huang<sup>4</sup>, G. S. Huang<sup>40</sup>, J. S. Huang<sup>12</sup>, L. Huang<sup>1</sup>, X. T. Huang<sup>28</sup>, Y. Huang<sup>24</sup>, Y. P. Huang<sup>1</sup>, T. Hussain<sup>42</sup>, C. S. Ji<sup>40</sup>,  
12 Q. Ji<sup>1</sup>, Q. P. Ji<sup>25</sup>, X. B. Ji<sup>1</sup>, X. L. Ji<sup>1</sup>, L. L. Jiang<sup>1</sup>, X. S. Jiang<sup>1</sup>, J. B. Jiao<sup>28</sup>, Z. Jiao<sup>14</sup>, D. P. Jin<sup>1</sup>, S. Jin<sup>1</sup>, F. F. Jing<sup>33</sup>,  
13 N. Kalantar-Nayestanaki<sup>20</sup>, M. Kavatsyuk<sup>20</sup>, B. Kopf<sup>2</sup>, M. Kornicer<sup>37</sup>, W. Kuehn<sup>35</sup>, W. Lai<sup>1</sup>, J. S. Lange<sup>35</sup>, P. Larin<sup>11</sup>,  
14 M. Leyhe<sup>2</sup>, C. H. Li<sup>1</sup>, Cheng Li<sup>40</sup>, Cui Li<sup>40</sup>, D. M. Li<sup>46</sup>, F. Li<sup>1</sup>, G. Li<sup>1</sup>, H. B. Li<sup>1</sup>, J. C. Li<sup>1</sup>, K. Li<sup>10</sup>, Lei Li<sup>1</sup>, Q. J. Li<sup>1</sup>,  
15 S. L. Li<sup>1</sup>, W. D. Li<sup>1</sup>, W. G. Li<sup>1</sup>, X. L. Li<sup>28</sup>, X. N. Li<sup>1</sup>, X. Q. Li<sup>25</sup>, X. R. Li<sup>27</sup>, Z. B. Li<sup>32</sup>, H. Liang<sup>40</sup>, Y. F. Liang<sup>30</sup>,  
16 Y. T. Liang<sup>35</sup>, G. R. Liao<sup>33</sup>, X. T. Liao<sup>1</sup>, D. Lin<sup>11</sup>, B. J. Liu<sup>1</sup>, C. L. Liu<sup>3</sup>, C. X. Liu<sup>1</sup>, F. H. Liu<sup>29</sup>, Fang Liu<sup>1</sup>, Feng Liu<sup>4</sup>,  
17 H. Liu<sup>1</sup>, H. B. Liu<sup>9</sup>, H. H. Liu<sup>13</sup>, H. M. Liu<sup>1</sup>, H. W. Liu<sup>1</sup>, J. P. Liu<sup>44</sup>, K. Liu<sup>33</sup>, K. Y. Liu<sup>22</sup>, Kai Liu<sup>36</sup>, P. L. Liu<sup>28</sup>, Q. Liu<sup>36</sup>,  
18 S. B. Liu<sup>40</sup>, X. Liu<sup>21</sup>, Y. B. Liu<sup>25</sup>, Z. A. Liu<sup>1</sup>, Zhiqiang Liu<sup>1</sup>, Zhiqing Liu<sup>1</sup>, H. Loehner<sup>20</sup>, G. R. Lu<sup>12</sup>, H. J. Lu<sup>14</sup>, J. G. Lu<sup>1</sup>,  
19 Q. W. Lu<sup>29</sup>, X. R. Lu<sup>36</sup>, Y. P. Lu<sup>1</sup>, C. L. Luo<sup>23</sup>, M. X. Luo<sup>45</sup>, T. Luo<sup>37</sup>, X. L. Luo<sup>1</sup>, M. Lv<sup>1</sup>, C. L. Ma<sup>36</sup>, F. C. Ma<sup>22</sup>,  
20 H. L. Ma<sup>1</sup>, Q. M. Ma<sup>1</sup>, S. Ma<sup>1</sup>, T. Ma<sup>1</sup>, X. Y. Ma<sup>1</sup>, F. E. Maas<sup>11</sup>, M. Maggiora<sup>43A,43C</sup>, Q. A. Malik<sup>42</sup>, Y. J. Mao<sup>26</sup>,  
21 Z. P. Mao<sup>1</sup>, J. G. Messchendorp<sup>20</sup>, J. Min<sup>1</sup>, T. J. Min<sup>1</sup>, R. E. Mitchell<sup>16</sup>, X. H. Mo<sup>1</sup>, H. Moeini<sup>20</sup>, C. Morales Morales<sup>11</sup>,  
22 K. Moriya<sup>16</sup>, N. Yu. Muchnoi<sup>6</sup>, H. Muramatsu<sup>39</sup>, Y. Nefedov<sup>19</sup>, C. Nicholson<sup>36</sup>, I. B. Nikolaev<sup>6</sup>, Z. Ning<sup>1</sup>, S. L. Olsen<sup>27</sup>,  
23 Q. Ouyang<sup>1</sup>, S. Pacetti<sup>17B</sup>, J. W. Park<sup>27</sup>, M. Pelizaeus<sup>2</sup>, H. P. Peng<sup>40</sup>, K. Peters<sup>7</sup>, J. L. Ping<sup>23</sup>, R. G. Ping<sup>1</sup>, R. Poling<sup>38</sup>,  
24 E. Prencipe<sup>18</sup>, M. Qi<sup>24</sup>, S. Qian<sup>1</sup>, C. F. Qiao<sup>36</sup>, L. Q. Qin<sup>28</sup>, X. S. Qin<sup>1</sup>, Y. Qin<sup>26</sup>, Z. H. Qin<sup>1</sup>, J. F. Qiu<sup>1</sup>, K. H. Rashid<sup>42</sup>,  
25 G. Rong<sup>1</sup>, X. D. Ruan<sup>9</sup>, A. Sarantsev<sup>19,c</sup>, B. D. Schaefer<sup>16</sup>, M. Shao<sup>40</sup>, C. P. Shen<sup>37,d</sup>, X. Y. Shen<sup>1</sup>, H. Y. Sheng<sup>1</sup>,  
26 M. R. Shepherd<sup>16</sup>, W. M. Song<sup>1</sup>, X. Y. Song<sup>1</sup>, S. Spataro<sup>43A,43C</sup>, B. Spruck<sup>35</sup>, D. H. Sun<sup>1</sup>, G. X. Sun<sup>1</sup>, J. F. Sun<sup>12</sup>, S. S. Sun<sup>1</sup>,  
27 Y. J. Sun<sup>40</sup>, Y. Z. Sun<sup>1</sup>, Z. J. Sun<sup>1</sup>, Z. T. Sun<sup>40</sup>, C. J. Tang<sup>30</sup>, X. Tang<sup>1</sup>, I. Tapan<sup>34C</sup>, E. H. Thorndike<sup>39</sup>, D. Toth<sup>38</sup>,  
28 M. Ullrich<sup>35</sup>, I. Uman<sup>34B</sup>, G. S. Varner<sup>37</sup>, B. Q. Wang<sup>26</sup>, D. Wang<sup>26</sup>, D. Y. Wang<sup>26</sup>, K. Wang<sup>1</sup>, L. L. Wang<sup>1</sup>, L. S. Wang<sup>1</sup>,  
29 M. Wang<sup>28</sup>, P. Wang<sup>1</sup>, P. L. Wang<sup>1</sup>, Q. J. Wang<sup>1</sup>, S. G. Wang<sup>26</sup>, X. F. Wang<sup>33</sup>, X. L. Wang<sup>40</sup>, Y. D. Wang<sup>17A</sup>, Y. F. Wang<sup>1</sup>,  
30 Y. Q. Wang<sup>18</sup>, Z. Wang<sup>1</sup>, Z. G. Wang<sup>1</sup>, Z. Y. Wang<sup>1</sup>, D. H. Wei<sup>8</sup>, J. B. Wei<sup>26</sup>, P. Weidenkaff<sup>18</sup>, Q. G. Wen<sup>40</sup>, S. P. Wen<sup>1</sup>,  
31 M. Werner<sup>35</sup>, U. Wiedner<sup>2</sup>, L. H. Wu<sup>1</sup>, N. Wu<sup>1</sup>, S. X. Wu<sup>40</sup>, W. Wu<sup>25</sup>, Z. Wu<sup>1</sup>, L. G. Xia<sup>33</sup>, Y. X. Xia<sup>15</sup>, Z. J. Xiao<sup>23</sup>,  
32 Y. G. Xie<sup>1</sup>, Q. L. Xiu<sup>1</sup>, G. F. Xu<sup>1</sup>, G. M. Xu<sup>26</sup>, Q. J. Xu<sup>10</sup>, Q. N. Xu<sup>36</sup>, X. P. Xu<sup>31</sup>, Z. R. Xu<sup>40</sup>, F. Xue<sup>4</sup>, Z. Xue<sup>1</sup>, L. Yan<sup>40</sup>,  
33 W. B. Yan<sup>40</sup>, Y. H. Yan<sup>15</sup>, H. X. Yang<sup>1</sup>, Y. Yang<sup>4</sup>, Y. X. Yang<sup>8</sup>, H. Ye<sup>1</sup>, M. Ye<sup>1</sup>, M. H. Ye<sup>5</sup>, B. X. Yu<sup>1</sup>, C. X. Yu<sup>25</sup>,  
34 H. W. Yu<sup>26</sup>, J. S. Yu<sup>21</sup>, S. P. Yu<sup>28</sup>, C. Z. Yuan<sup>1</sup>, Y. Yuan<sup>1</sup>, A. A. Zafar<sup>42</sup>, A. Zallo<sup>17A</sup>, S. L. Zang<sup>24</sup>, Y. Zeng<sup>15</sup>, B. X. Zhang<sup>1</sup>,  
35 B. Y. Zhang<sup>1</sup>, C. Zhang<sup>24</sup>, C. C. Zhang<sup>1</sup>, D. H. Zhang<sup>1</sup>, H. H. Zhang<sup>32</sup>, H. Y. Zhang<sup>1</sup>, J. Q. Zhang<sup>1</sup>, J. W. Zhang<sup>1</sup>,  
36 J. Y. Zhang<sup>1</sup>, J. Z. Zhang<sup>1</sup>, LiLi Zhang<sup>15</sup>, R. Zhang<sup>36</sup>, S. H. Zhang<sup>1</sup>, X. J. Zhang<sup>1</sup>, X. Y. Zhang<sup>28</sup>, Y. Zhang<sup>1</sup>, Y. H. Zhang<sup>1</sup>,  
37 Z. P. Zhang<sup>40</sup>, Z. Y. Zhang<sup>44</sup>, Zhenghao Zhang<sup>4</sup>, G. Zhao<sup>1</sup>, H. S. Zhao<sup>1</sup>, J. W. Zhao<sup>1</sup>, K. X. Zhao<sup>23</sup>, Lei Zhao<sup>40</sup>, Ling Zhao<sup>1</sup>,  
38 M. G. Zhao<sup>25</sup>, Q. Zhao<sup>1</sup>, S. J. Zhao<sup>46</sup>, T. C. Zhao<sup>1</sup>, X. H. Zhao<sup>24</sup>, Y. B. Zhao<sup>1</sup>, Z. G. Zhao<sup>40</sup>, A. Zhemchugov<sup>19,a</sup>, B. Zheng<sup>41</sup>,  
39 J. P. Zheng<sup>1</sup>, Y. H. Zheng<sup>36</sup>, B. Zhong<sup>23</sup>, L. Zhou<sup>1</sup>, X. Zhou<sup>44</sup>, X. K. Zhou<sup>36</sup>, X. R. Zhou<sup>40</sup>, C. Zhu<sup>1</sup>, K. Zhu<sup>1</sup>, K. J. Zhu<sup>1</sup>,  
40 S. H. Zhu<sup>1</sup>, X. L. Zhu<sup>33</sup>, Y. C. Zhu<sup>40</sup>, Y. M. Zhu<sup>25</sup>, Y. S. Zhu<sup>1</sup>, Z. A. Zhu<sup>1</sup>, J. Zhuang<sup>1</sup>, B. S. Zou<sup>1</sup>, J. H. Zou<sup>1</sup>

(BESIII Collaboration)

<sup>1</sup> Institute of High Energy Physics, Beijing 100049, People's Republic of China<sup>2</sup> Bochum Ruhr-University, D-44780 Bochum, Germany<sup>3</sup> Carnegie Mellon University, Pittsburgh, Pennsylvania 15213, USA<sup>4</sup> Central China Normal University, Wuhan 430079, People's Republic of China<sup>5</sup> China Center of Advanced Science and Technology, Beijing 100190, People's Republic of China<sup>6</sup> G.I. Budker Institute of Nuclear Physics SB RAS (BINP), Novosibirsk 630090, Russia<sup>7</sup> GSI Helmholtzcentre for Heavy Ion Research GmbH, D-64291 Darmstadt, Germany<sup>8</sup> Guangxi Normal University, Guilin 541004, People's Republic of China<sup>9</sup> GuangXi University, Nanning 530004, People's Republic of China<sup>10</sup> Hangzhou Normal University, Hangzhou 310036, People's Republic of China<sup>11</sup> Helmholtz Institute Mainz, Johann-Joachim-Becher-Weg 45, D-55099 Mainz, Germany<sup>12</sup> Henan Normal University, Xinxiang 453007, People's Republic of China<sup>13</sup> Henan University of Science and Technology, Luoyang 471003, People's Republic of China<sup>14</sup> Huangshan College, Huangshan 245000, People's Republic of China<sup>15</sup> Hunan University, Changsha 410082, People's Republic of China<sup>16</sup> Indiana University, Bloomington, Indiana 47405, USA<sup>17</sup> (A)INFN Laboratori Nazionali di Frascati, I-00044, Frascati,

Italy; (B)INFN and University of Perugia, I-06100, Perugia, Italy

<sup>18</sup> Johannes Gutenberg University of Mainz, Johann-Joachim-Becher-Weg 45, D-55099 Mainz, Germany<sup>19</sup> Joint Institute for Nuclear Research, 141980 Dubna, Moscow region, Russia

- 62 <sup>20</sup> *KVI, University of Groningen, NL-9747 AA Groningen, The Netherlands*  
63 <sup>21</sup> *Lanzhou University, Lanzhou 730000, People's Republic of China*  
64 <sup>22</sup> *Liaoning University, Shenyang 110036, People's Republic of China*  
65 <sup>23</sup> *Nanjing Normal University, Nanjing 210023, People's Republic of China*  
66 <sup>24</sup> *Nanjing University, Nanjing 210093, People's Republic of China*  
67 <sup>25</sup> *Nankai University, Tianjin 300071, People's Republic of China*  
68 <sup>26</sup> *Peking University, Beijing 100871, People's Republic of China*  
69 <sup>27</sup> *Seoul National University, Seoul, 151-747 Korea*  
70 <sup>28</sup> *Shandong University, Jinan 250100, People's Republic of China*  
71 <sup>29</sup> *Shanxi University, Taiyuan 030006, People's Republic of China*  
72 <sup>30</sup> *Sichuan University, Chengdu 610064, People's Republic of China*  
73 <sup>31</sup> *Soochow University, Suzhou 215006, People's Republic of China*  
74 <sup>32</sup> *Sun Yat-Sen University, Guangzhou 510275, People's Republic of China*  
75 <sup>33</sup> *Tsinghua University, Beijing 100084, People's Republic of China*  
76 <sup>34</sup> (A) *Ankara University, Dogol Caddesi, 06100 Tandogan, Ankara, Turkey; (B) Dogus*  
77 *University, 34722 Istanbul, Turkey; (C) Uludag University, 16059 Bursa, Turkey*  
78 <sup>35</sup> *Universitaet Giessen, D-35392 Giessen, Germany*  
79 <sup>36</sup> *University of Chinese Academy of Sciences, Beijing 100049, People's Republic of China*  
80 <sup>37</sup> *University of Hawaii, Honolulu, Hawaii 96822, USA*  
81 <sup>38</sup> *University of Minnesota, Minneapolis, Minnesota 55455, USA*  
82 <sup>39</sup> *University of Rochester, Rochester, New York 14627, USA*  
83 <sup>40</sup> *University of Science and Technology of China, Hefei 230026, People's Republic of China*  
84 <sup>41</sup> *University of South China, Hengyang 421001, People's Republic of China*  
85 <sup>42</sup> *University of the Punjab, Lahore-54590, Pakistan*  
86 <sup>43</sup> (A) *University of Turin, I-10125, Turin, Italy; (B) University of Eastern*  
87 *Piedmont, I-15121, Alessandria, Italy; (C) INFN, I-10125, Turin, Italy*  
88 <sup>44</sup> *Wuhan University, Wuhan 430072, People's Republic of China*  
89 <sup>45</sup> *Zhejiang University, Hangzhou 310027, People's Republic of China*  
90 <sup>46</sup> *Zhengzhou University, Zhengzhou 450001, People's Republic of China*
- 91 <sup>a</sup> *Also at the Moscow Institute of Physics and Technology, Moscow 141700, Russia*  
92 <sup>b</sup> *On leave from the Bogolyubov Institute for Theoretical Physics, Kiev 03680, Ukraine*  
93 <sup>c</sup> *Also at the PNPI, Gatchina 188300, Russia*  
94 <sup>d</sup> *Present address: Nagoya University, Nagoya 464-8601, Japan*  
95 (Dated: October 1, 2018)

The decay  $J/\psi \rightarrow \omega p\bar{p}$  has been studied, using  $225.3 \times 10^6$   $J/\psi$  events accumulated at BESIII. No significant enhancement near the  $p\bar{p}$  invariant-mass threshold (denoted as  $X(p\bar{p})$ ) is observed. The upper limit of the branching fraction  $\mathcal{B}(J/\psi \rightarrow \omega X(p\bar{p}) \rightarrow \omega p\bar{p})$  is determined to be  $3.9 \times 10^{-6}$  at the 95% confidence level. The branching fraction of  $J/\psi \rightarrow \omega p\bar{p}$  is measured to be  $\mathcal{B}(J/\psi \rightarrow \omega p\bar{p}) = (9.0 \pm 0.2 \text{ (stat.)} \pm 0.9 \text{ (syst.)}) \times 10^{-4}$ .

PACS numbers: 13.25.Gv, 12.39.Mk, 13.75.Cs

## I. INTRODUCTION

98 An anomalous enhancement near the threshold of the  
99  $p\bar{p}$  system, namely  $X(p\bar{p})$ , was first observed by the BE-  
100 SII experiment in the radiative decay  $J/\psi \rightarrow \gamma p\bar{p}$  [1],  
101 and it was recently confirmed by the CLEO and BESIII  
102 experiments [2–4]. In the BESII experiment, its mass is  
103 measured to be  $1859^{+3}_{-10}$  (stat.) $^{+5}_{-25}$  (syst.) MeV/ $c^2$  and  
104 the total width is  $\Gamma < 30$  MeV/ $c^2$  at the 90% confi-  
105 dence level (C.L.). While in the BESIII experiment, a  
106 partial wave analysis (PWA) with a correction for the  
107 final-state interaction (FSI) is performed, and the spin-  
108 parity of  $X(p\bar{p})$  is determined to be  $0^{-+}$ , its mass is  
109  $1832^{+19}_{-5}$  (stat.) $^{+18}_{-17}$  (syst.) MeV/ $c^2$  and the total width  
110 is  $\Gamma < 76$  MeV/ $c^2$  at the 90% C.L. [3].

111 The discovery of  $X(p\bar{p})$  stimulated a number of the-  
112 oretical interpretations and experimental studies [5–16].  
113 There is no experimental evidence of such an enhance-

114 ment in other quarkonium decays, e.g.  $J/\psi \rightarrow \pi^0 p\bar{p}$  [1]  
115 or  $\Upsilon(2S) \rightarrow \gamma p\bar{p}$  [5]. In  $\psi(2S) \rightarrow \gamma p\bar{p}$ , the recent BESIII  
116 measurement shows a relative production rate to that of  
117  $J/\psi$  decays of  $R = 5.08\%$  [3]. A number of theoretical  
118 speculations have been proposed to interpret the nature  
119 of this structure, including baryonium [9–11], a multi-  
120 quark state [12] or mainly a pure FSI [13, 14]. It was  
121 proposed to associate this enhancement with a broad en-  
122 hancement observed in  $B$  meson decays [17, 18] or a new  
123 resonance  $X(1835)$  in  $J/\psi \rightarrow \gamma \pi^+ \pi^- \eta'$  decay at BE-  
124 SII [19].

125 The investigation of the near-threshold  $p\bar{p}$  invariant  
126 mass spectrum in other  $J/\psi$  decay modes will be helpful  
127 in understanding the nature of the observed structure.  
128 The decay  $J/\psi \rightarrow \omega p\bar{p}$  restricts the isospin of the  $p\bar{p}$   
129 system, and it is helpful to clarify the role of the  $p\bar{p}$   
130 FSI. The BESII collaboration studied  $J/\psi \rightarrow \omega p\bar{p}$  via  $\omega$   
131 decaying to  $\pi^0 \pi^+ \pi^-$  with a data sample of  $5.8 \times 10^7$   $J/\psi$

132 events [6]. No significant signal near the threshold of the  
 133  $p\bar{p}$  invariant-mass spectrum was observed and an upper  
 134 limit on the branching fraction of  $J/\psi \rightarrow \omega X(p\bar{p}) \rightarrow \omega p\bar{p}$   
 135 was determined to be  $1.5 \times 10^{-5}$  at the 90% C.L., which  
 136 disfavored the interpretation of a pure FSI effect giving  
 137 rise to the  $X(p\bar{p})$ . In this paper, the analysis of  $J/\psi \rightarrow$   
 138  $\omega p\bar{p}$  via the decay channel  $\omega \rightarrow \gamma\pi^0$  is presented, based  
 139 on a data sample of  $(225.3 \pm 2.8) \times 10^6$   $J/\psi$  events [20]  
 140 accumulated with the BESIII detector. Searching for the  
 141  $X(p\bar{p})$  in the decay mode  $J/\psi \rightarrow \omega p\bar{p} \rightarrow \gamma\pi^0 p\bar{p}$  has a  
 142 particular advantage: a low irreducible background from  
 143  $N^*$  is expected. The channel  $J/\psi \rightarrow \omega p\bar{p} \rightarrow \pi\pi\pi^0 p\bar{p}$  has  
 144 irreducible background from various  $N^*$  decays and  $\Delta$   
 145 decays, where interferences may have a large impact on  
 146 the uncertainty of the measurements.

147 BESIII/BEPCII [21] is a major upgrade of the BESII  
 148 experiment at the BEPC accelerator [22] for studies of  
 149 hadron spectroscopy and  $\tau$ -charm physics [23]. The de-  
 150 sign peak luminosity of the double-ring  $e^+e^-$  collider,  
 151 BEPCII, is  $10^{33} \text{ cm}^{-2}\text{s}^{-1}$  at beam currents of 0.93 A. The  
 152 BESIII detector with a geometrical acceptance of 93%  
 153 of  $4\pi$ , consists of the following main components: 1) a  
 154 small-celled, helium-based main drift chamber (MDC)  
 155 with 43 layers. The average single wire resolution is  
 156  $135 \mu\text{m}$ , and the momentum resolution for  $1 \text{ GeV}/c^2$   
 157 charged particles in a 1 T magnetic field is 0.5%; 2)  
 158 an electromagnetic calorimeter (EMC) made of 6240  
 159 CsI(Tl) crystals arranged in a cylindrical shape (barrel)  
 160 plus two end-caps. For 1.0 GeV photons, the energy res-  
 161 olution is 2.5% in the barrel and 5% in the end-caps, and  
 162 the position resolution is 6 mm in the barrel and 9 mm in  
 163 the end-caps; 3) a Time-Of-Flight system (TOF) for par-  
 164 ticle identification (PID) composed of a barrel part made  
 165 of two layers with 88 pieces of 5 cm thick, 2.4 m long plas-  
 166 tic scintillators in each layer, and two end-caps with 48  
 167 fan-shaped, 5 cm thick, plastic scintillators in each end-  
 168 cap. The time resolution is 80 ps in the barrel, and 110  
 169 ps in the end-caps, corresponding to a  $K/\pi$  separation  
 170 by more than  $2\sigma$  for momenta below about  $1 \text{ GeV}/c^2$ ;  
 171 4) a muon chamber system (MUC) made of  $1000 \text{ m}^2$  of  
 172 Resistive Plate Chambers (RPC) arranged in 9 layers in  
 173 the barrel and 8 layers in the end-caps and incorporated  
 174 in the return iron yoke of the superconducting magnet.  
 175 The position resolution is about 2 cm.

176 The optimization of the event selection and the es-  
 177 timate of physics backgrounds are performed through  
 178 Monte Carlo (MC) simulations. The GEANT4-based  
 179 simulation software BOOST [24] includes the geometric  
 180 and material description of the BESIII detectors and the  
 181 detector response and digitization models, as well as the  
 182 tracking of the detector running conditions and perfor-  
 183 mance. The production of the  $J/\psi$  resonance is simu-  
 184 lated by the MC event generator KKMC [25], while the  
 185 decays are generated by EVTGEN [26] for known de-  
 186 cay modes with branching ratios being set to PDG [27]  
 187 world average values, and by LUNDCHARM [28] for the  
 188 remaining unknown decays. The analysis is performed in  
 189 the framework of the BESIII offline software system [29]

190 which takes care of the detector calibration, event recon-  
 191 struction and data storage.

## 192 II. EVENT SELECTION

193 Signal  $J/\psi \rightarrow \omega p\bar{p}$  events with  $\omega \rightarrow \gamma\pi^0$  final states  
 194 have the topology  $\gamma\gamma p\bar{p}$ . The event candidates are re-  
 195 quired to have two well reconstructed charged tracks with  
 196 net charge zero, and at least three photons.

197 Charged-particle tracks in the polar angle range  
 198  $|\cos\theta| < 0.93$  are reconstructed from the MDC hits, only  
 199 tracks in barrel region ( $|\cos\theta| < 0.8$ ) are used to reduce  
 200 systematic uncertainties in tracking and particle identi-  
 201 fication. Tracks with their points of closest approach to  
 202 the beamline within  $\pm 10 \text{ cm}$  of the interaction point in  
 203 the beam direction, and within 1 cm in the plane perpen-  
 204 dicular to the beam are selected. TOF and  $dE/dx$  infor-  
 205 mation are combined to determine particle identification  
 206 confidence levels for  $\pi$ ,  $K$  and  $p(\bar{p})$  hypotheses; and the  
 207 particle type with highest confidence level is assigned to  
 208 each track. A proton and an anti-proton are required.  
 209 To reduce the systematic error due to differences of the  
 210 tracking efficiency at low momentum between data and  
 211 MC, the momentum of the proton or anti-proton is fur-  
 212 ther required to be larger than  $300 \text{ MeV}/c$ .

213 Photon candidates are reconstructed by clustering sig-  
 214 nals in EMC crystals. The photon candidates are re-  
 215 quired to be in the barrel region ( $|\cos\theta| < 0.8$ ) of the  
 216 EMC with at least 25 MeV energy deposition, or in the  
 217 end-caps region ( $0.86 < |\cos\theta| < 0.92$ ) with at least  
 218 50 MeV energy deposition, where  $\theta$  is the polar angle of  
 219 the shower. Timing information from the EMC is used to  
 220 suppress electronic noise and energy depositions that are  
 221 unrelated to the event. To suppress showers generated by  
 222 charged particles, the photon candidates are furthermore  
 223 required to be separated by an angle larger than  $10^\circ$  and  
 224 larger than  $30^\circ$  from the proton and anti-proton, respec-  
 225 tively.

226 A four-constraint (4C) energy-momentum conserving  
 227 kinematic fit is performed to the  $\gamma\gamma p\bar{p}$  hypothesis. For  
 228 events with more than three photon candidates, the com-  
 229 bination with the minimum  $\chi_{4C}^2$  is selected, and  $\chi_{4C}^2 < 30$   
 230 is required. The  $\pi^0$  candidates are reconstructed from the  
 231 two of the three selected photons with an invariant mass  
 232 closest to the  $\pi^0$  mass, and  $|M_{\gamma\gamma} - M_{\pi^0}| < 15 \text{ MeV}/c^2$  is  
 233 required.

## 234 III. BRANCHING FRACTION AND YIELD 235 MEASUREMENTS

236  
 237 Figure 1 shows the  $\gamma\pi^0$  invariant mass spectrum for  
 238 candidate  $J/\psi \rightarrow \gamma\pi^0 p\bar{p}$  events, where a distinctive  $\omega$   
 239 signal is seen. An unbinned maximum likelihood fit is  
 240 performed to the  $\gamma\pi^0$  invariant mass with the  $\omega$  signal

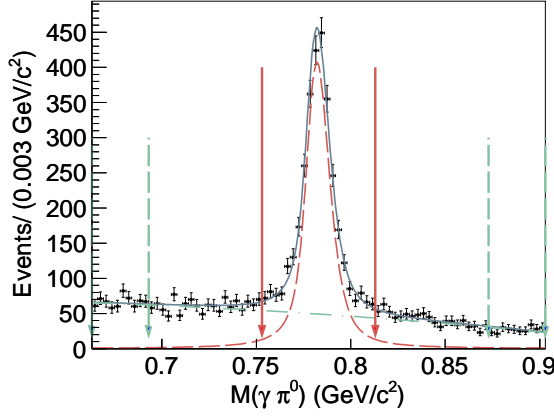


FIG. 1.  $\gamma\pi^0$  invariant mass distribution of  $J/\psi \rightarrow \gamma\pi^0 p\bar{p}$  candidates. The dashed line is the signal shape which is parametrized by a Breit-Wigner function convoluted with the detector resolution described by the Novosibirsk function; the dashed-dotted line is the background shape which is described by a second order Chebychev polynomial; and the solid line is the total contribution of the two components. The solid arrows indicate the  $\omega$  signal region ( $0.753 < M(\gamma\pi^0) < 0.813 \text{ GeV}/c^2$ ) and the two pairs of dashed arrows indicate the  $\omega$  sidebands ( $0.663 < M(\gamma\pi^0) < 0.693 \text{ GeV}/c^2$  and  $0.873 < M(\gamma\pi^0) < 0.903 \text{ GeV}/c^2$ ).

241 parametrized by a Breit-Wigner function convoluted with  
 242 the Novosibirsk function [30] which describes the detec-  
 243 tor resolution. The background shape is described by a  
 244 second-order Chebychev polynomial function. The mass  
 245 and width of the  $\omega$  peak are fixed to the values published  
 246 by the Particle Data Group (PDG) [27], and the yield of  
 247 the  $\omega$  signal obtained from the fit is  $N_{obs} = 2670 \pm 69$ .

248 The branching fraction of  $J/\psi \rightarrow \omega p\bar{p}$  is calculated  
 249 according to :

$$\mathcal{B}(J/\psi \rightarrow \omega p\bar{p}) = \frac{N_{obs}}{N_{J/\psi} \times \mathcal{B}(\omega \rightarrow \gamma\pi^0) \times \mathcal{B}(\pi^0 \rightarrow \gamma\gamma) \times \varepsilon_{rec}}. \quad (1)$$

250 where  $N_{obs}$  is the number of signal events determined  
 251 from the fit to the  $\gamma\pi^0$  invariant mass;  $N_{J/\psi}$  is the num-  
 252 ber of  $J/\psi$  events [20];  $\mathcal{B}(\omega \rightarrow \gamma\pi^0)$  and  $\mathcal{B}(\pi^0 \rightarrow \gamma\gamma)$   
 253 are branching fractions of  $\omega \rightarrow \gamma\pi^0$  and  $\pi^0 \rightarrow \gamma\gamma$ , re-  
 254 spectively, as from the PDG [27]; and the detection effi-  
 255 ciency  $\varepsilon_{rec}$  is  $(16.1 \pm 1.7)\%$  obtained from a MC sample  
 256 for  $J/\psi \rightarrow \omega p\bar{p}$  events generated according to a phase-  
 257 space distribution. The measured branching fraction is  
 258  $\mathcal{B}(J/\psi \rightarrow \omega p\bar{p}) = (9.0 \pm 0.2 \text{ (stat.)}) \times 10^{-4}$ .

259 Candidate  $J/\psi \rightarrow \omega p\bar{p}$  events are selected with the  
 260 mass window requirement  $0.753 \text{ GeV}/c^2 < M(\gamma\pi^0) <$   
 261  $0.813 \text{ GeV}/c^2$ , and the Dalitz plot of these events is shown  
 262 in Fig. 2. There are no obvious structures in the Dalitz  
 263 plot, though the distribution is different from the pure  
 264  $\omega p\bar{p}$  phase space distribution. The corresponding  $p\bar{p}$ ,  
 265  $\omega p$  and  $\omega\bar{p}$  invariant-mass spectra are also presented in  
 266 Fig. 2. The data points with error bars are from signal  
 267 region and the hatched area are from the sideband region.  
 268 the mass threshold is shown in Fig. 3.

269 To obtain the number of  $J/\psi \rightarrow \omega X(p\bar{p}) \rightarrow \omega p\bar{p}$   
 270 events, an unbinned maximum likelihood fit is performed  
 271 to the  $p\bar{p}$  invariant mass around the mass threshold. In  
 272 the fit, the spin-parity of  $X(p\bar{p})$  is assumed to be  $0^-$ ,  
 273 and the signal of  $X(p\bar{p})$  in the  $J/\psi \rightarrow \omega X(p\bar{p}) \rightarrow \omega p\bar{p}$   
 274 decay is parametrized by an acceptance-weighted  $\mathcal{S}$ -wave  
 275 Breit-Wigner function :

$$BW(M) \simeq \frac{q^{2L+1} k^3}{(M^2 - M_0^2)^2 + M_0^2 \Gamma^2} \times \varepsilon_{rec}(M). \quad (2)$$

276 Here,  $q$  is the momentum of the proton in the  $p\bar{p}$  rest  
 277 frame;  $k$  is the the momentum of the  $\omega$  meson;  $L = 0$   
 278 is the relative orbital angular momentum;  $M$  is the in-

279 variant mass of  $p\bar{p}$ ;  $M_0$  and  $\Gamma$  are the mass and width  
 280 of the  $X(p\bar{p})$ , respectively, which are taken from BESII  
 281 II results [3];  $\varepsilon_{rec}$  is the detection efficiency. The non-  
 282  $\omega$  background is presented by a function of the form  
 283  $f(\delta) = N(\delta^{1/2} + a_1 \delta^{3/2} + a_2 \delta^{5/2})$  with  $\delta = M_{p\bar{p}} - 2m_p$   
 284 where  $m_p$  is the proton mass. The normalization and  
 285 shape parameters  $a_1$  and  $a_2$  are determined by a simulta-  
 286 neous fit to the  $M(p\bar{p})$  in  $\omega$  signal region and  $\omega$  sideband  
 287 region  $0.09 \text{ GeV}/c^2 < |M(\gamma\pi^0) - 0.783| < 0.12 \text{ GeV}/c^2$ .  
 288 The non-resonant  $J/\psi \rightarrow \omega p\bar{p}$  events are also described  
 289 by the function  $f(\delta)$ , where the normalization and shape  
 290 parameters are allowed to float. The fit results are shown  
 291 in Fig. 3, and the number of  $X(p\bar{p})$  events is  $0 \pm 1.6$ .  
 292 A Bayesian approach [27] estimate the upper limit of  
 293  $\mathcal{B}(J/\psi \rightarrow \omega X(p\bar{p}) \rightarrow \omega p\bar{p})$ , and  $N_{obs} < 9$  at 95% C.  
 294 L. is determined by finding the value  $N_{obs}^{UP}$  with

$$\frac{\int_0^{N_{obs}^{UP}} \mathcal{L} dN_{obs}}{\int_0^{\infty} \mathcal{L} dN_{obs}} = 0.95, \quad (3)$$

295 where  $N_{obs}$  is the number of signal events, and  $\mathcal{L}$  is the  
 296 value of the likelihood function with the  $N_{obs}$  value fixed  
 297 in the fit. The upper limit on the product of branching  
 298 fractions is calculated with

$$\mathcal{B}(J/\psi \rightarrow \omega X(p\bar{p}) \rightarrow \omega p\bar{p}) < \frac{N_{obs}^{UL}}{N_{J/\psi} \times (1 - \sigma_{sys.}) \times \mathcal{B}(\omega \rightarrow \gamma\pi^0) \times \mathcal{B}(\pi^0 \rightarrow \gamma\gamma) \times \varepsilon_{rec}}, \quad (4)$$

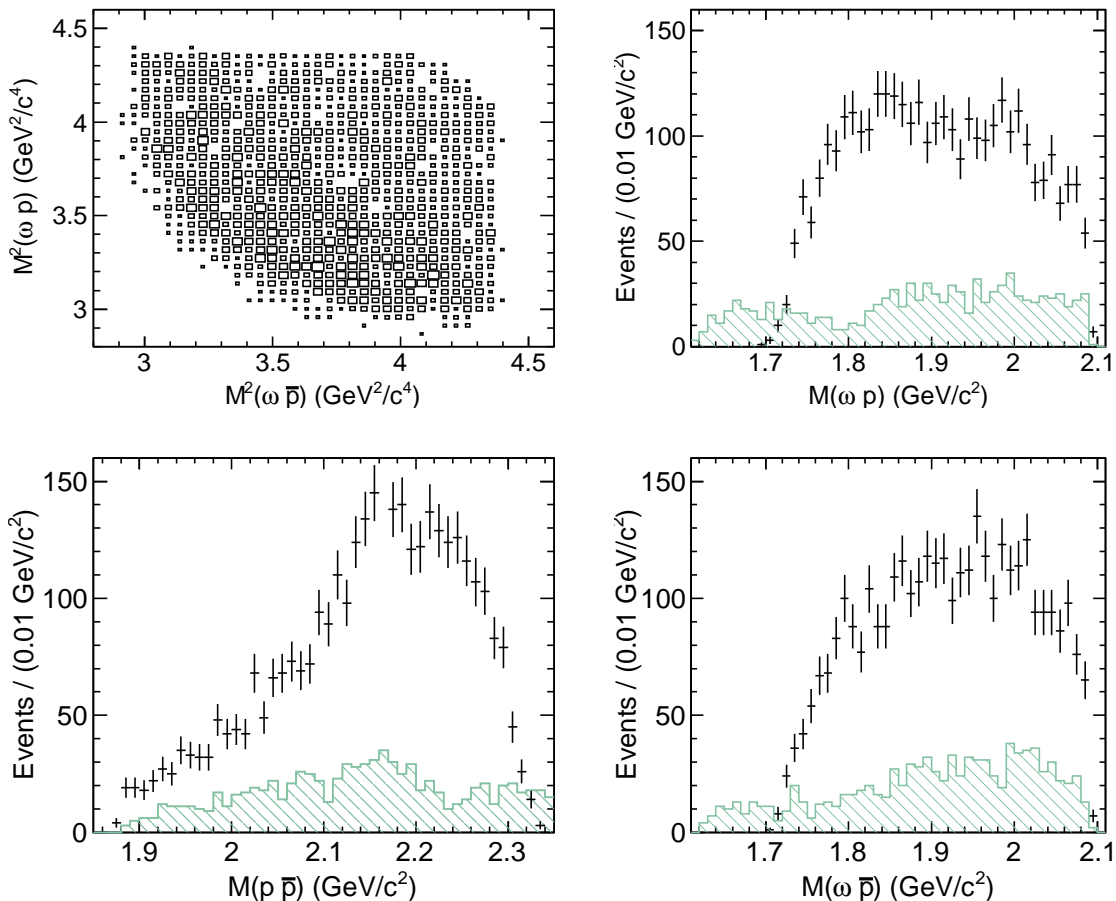


FIG. 2. Dalitz plot and  $p\bar{p}$ ,  $\omega p$ ,  $\omega\bar{p}$  invariant-mass spectra of  $J/\psi \rightarrow \omega p\bar{p}$  candidates. The data points with error bars are from signal region and the hatched areas are from the sideband region.

299 where  $\sigma_{sys.}$  is the total systematic uncertainty which will  
 300 be described in the next section. The upper limit on the  
 301 product of branching fractions is  $\mathcal{B}(J/\psi \rightarrow \omega X(p\bar{p}) \rightarrow$   
 302  $\omega p\bar{p}) < 3.9 \times 10^{-6}$  at the 95% C.L..

303 An alternative fit with a Breit-Wigner function includ-  
 304 ing the Jülich FSI

$$BW(M) \simeq \frac{f_{FSI} \times q^{2L+1} k^3}{(M^2 - M_0^2)^2 + M_0^2 \Gamma^2} \times \varepsilon_{rec}(M), \quad (5)$$

305 for  $X(p\bar{p})$  is performed. Here,  $f_{FSI}$  is the Jülich FSI cor-  
 306 rection factor [14]. The mass and width of  $X(p\bar{p})$  are  
 307 taken from the previous BESIII PWA results [3]. The  
 308 upper limit on the product of branching fractions is de-  
 309 termined to be  $\mathcal{B}(J/\psi \rightarrow \omega X(p\bar{p}) \rightarrow \omega p\bar{p}) < 3.7 \times 10^{-6}$   
 310 at the 95% C.L..

#### IV. SYSTEMATIC UNCERTAINTIES

312 Several sources of systematic uncertainties are con-  
 313 sidered in the measurement of the branching fractions.  
 314 These include differences between data and the MC sim-  
 315 ulation for the tracking algorithm, the PID, photon de-  
 316 tection, the kinematic fit, as well as the fitting procedure,  
 317 the branching fraction of the intermediate states and the  
 318 total number of  $J/\psi$  events.

319 The systematic uncertainties associated with the track-  
 320 ing efficiency and PID efficiency have been studied with  
 321  $J/\psi \rightarrow p\bar{p}\pi^+\pi^-$  using a technique similar to that dis-  
 322 cussed in Ref. [31]. The difference of tracking efficiencies  
 323 between data and MC simulation is 2% per charged track.  
 324 The systematic uncertainty from PID is 2% per proton  
 325 (anti-proton).

326 The photon detection systematic uncertainty is studied  
 327 by comparing the photon efficiency between MC simula-  
 328 tion and the control sample  $J/\psi \rightarrow \rho\pi$ . The relative  
 329 efficiency difference is about 1% for each photon [32, 33].

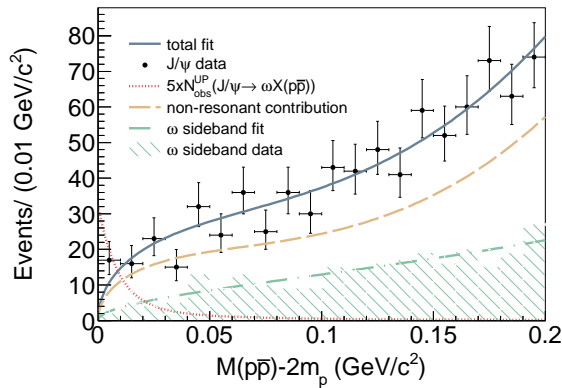


FIG. 3. Near-threshold  $p\bar{p}$  invariant-mass spectrum. The signal  $J/\psi \rightarrow \omega X(p\bar{p}) \rightarrow \omega p\bar{p}$  is described by an acceptance-weighted Breit-Wigner function, and signal yield is consistent with zero. The dotted line is the shape of the signal which is normalized to five times the estimated upper limit. The dashed line is the non-resonant contribution described by the function  $f(\delta)$  and the dashed-dotted line is the non  $\omega p\bar{p}$  contribution which is estimated from  $\omega$  sidebands. The solid line is the total contribution of the two components. The hatched area is from the sideband region.

330 Here, 3% is taken as the systematic error for the efficiency of detecting three photons. The uncertainty due to  $\pi^0$  reconstruction efficiency is taken as 1% [32, 33].

333 To estimate the uncertainty associated with the kinematic fit, selected samples of  $J/\psi \rightarrow \Sigma^+ \bar{\Sigma}^- \rightarrow p\pi^0 \bar{p}\pi^0$  events are used. The kinematic fit efficiency is defined as the ratio between the signal yield of  $\Sigma^+$  with or without the kinematic fit. The difference of kinematic fit efficiency between data and MC is 3%, and is taken as the systematic uncertainty caused by the kinematic fit.

340 As described above, the yield of  $J/\psi \rightarrow \omega p\bar{p}$  is derived from a fit to the invariant-mass spectrum of  $\gamma\pi^0$  pairs. To evaluate the systematic uncertainty associated with the fitting procedure, the following two aspects are studied (i) *Fitting region*: In the nominal fit, the mass spectrum of  $\gamma\pi^0$  is fitted in the range from 0.663  $\text{GeV}/c^2$  to 0.903  $\text{GeV}/c^2$ . Alternative fits within ranges 0.653  $\text{GeV}/c^2$  to 0.913  $\text{GeV}/c^2$  and 0.673  $\text{GeV}/c^2$  to 0.893  $\text{GeV}/c^2$  are performed, and the difference in the signal yield of 2% is taken as the systematic uncertainty associated with the fit interval. (ii) *Background shape*: To estimate the uncertainty due to the background parametrization for the branching fraction  $\mathcal{B}(J/\psi \rightarrow \omega p\bar{p})$ , a first or third order instead of a second-order Chebychev polynomial is used in the fitting. The difference of 1.2% is used as an estimate of the systematic uncertainty.

357 For the upper limit on the branching fraction  $\mathcal{B}(J/\psi \rightarrow$

358  $\omega X(p\bar{p}) \rightarrow \omega p\bar{p}$ ), the systematic uncertainty associated with the fitting procedure is estimated by fixing the shape of the non-resonant contribution to a phase space MC simulation of  $J/\psi \rightarrow \omega p\bar{p}$ , which is pre-

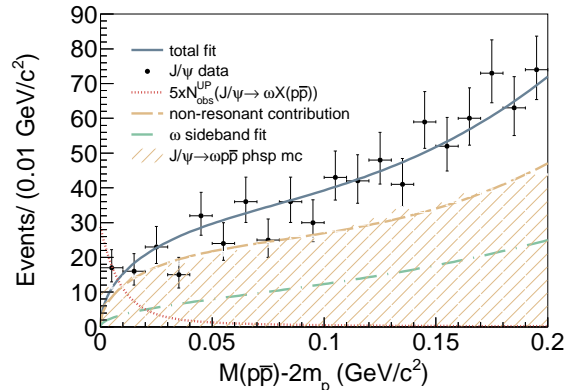


FIG. 4. Near-threshold  $p\bar{p}$  invariant-mass spectrum. The signal  $J/\psi \rightarrow \omega X(p\bar{p}) \rightarrow \omega p\bar{p}$  is described by an acceptance-weighted Breit-Wigner function, and signal yield is consistent with zero. The dashed line is the non-resonant contribution fixed to a phase space MC simulation of  $J/\psi \rightarrow \omega p\bar{p}$  and the dashed-dotted line is the non  $\omega p\bar{p}$  contribution which is estimated from  $\omega$  sidebands. The solid line is the total contribution of the two components. The hatched area is from a phase space MC simulation of  $J/\psi \rightarrow \omega p\bar{p}$ .

362 sent by Figure. 4; enlarging/reducing the normaliza-  
363 tion of the non- $\omega$  contribution by 7% (the difference of  
364 the estimation of non- $\omega$  background level between data  
365 and inclusive MC); and varying the sideband region  
366 to  $0.095 \text{ GeV}/c^2 < |M(\gamma\pi^0) - 0.783| < 0.115 \text{ GeV}/c^2$   
367 and  $0.085 \text{ GeV}/c^2 < |M(\gamma\pi^0) - 0.783| < 0.125 \text{ GeV}/c^2$ .  
368 When fitting with or without the FSI effect, the signal  
369 yields for the alternative fits are lower or equal to the  
370 nominal fit, therefore the conservative upper limit from  
371 the fit without FSI correction is reported.

372 Various distributions obtained with data and the  
373 phase-space MC sample have been compared and some  
374 discrepancies are observed. To determine the systematic  
375 error on the detection efficiency associated with these  
376 discrepancies, an alternative detection efficiency is esti-  
377 mated by the re-weighting phase-space MC samples. The  
378 difference in detection efficiency compared to the nomi-  
379 nal one is 7% and taken as a systematic uncertainty. The  
380 number of  $J/\psi$  events is determined from an inclusive  
381 analysis of  $J/\psi$  hadronic events and an uncertainty of  
382 1.24% is associated to it [20]. The uncertainties due to  
383 the branching fractions of  $\omega \rightarrow \gamma\pi^0$  and  $\pi^0 \rightarrow \gamma\gamma$  are  
384 taken from the PDG [27].

TABLE I. Summary of systematic uncertainties. '-' means the corresponding systematic uncertainty is negligible.

Source	$\mathcal{B}(J/\psi \rightarrow \omega p\bar{p})$	Upper limit of $\mathcal{B}(J/\psi \rightarrow \omega X(p\bar{p}) \rightarrow \omega p\bar{p})$	Upper limit of $\mathcal{B}(J/\psi \rightarrow \omega X(p\bar{p}) \rightarrow \omega p\bar{p})$ with FSI
Tracking	4%	4%	4%
PID	4%	4%	4%
Photon	3%	3%	3%
Kinematic Fit	3%	3%	3%
$\pi^0$ reconstruction	1%	1%	1%
Fitting region	2%	—	—
Background Shape	1%	—	—
Branching fraction of intermediate state	3%	3%	3%
Total $J/\psi$ numbers	1.24%	1.24%	1.24%
MC Generator	7%	—	—
Total uncertainty	10.3%	7.8%	7.8%

## V. SUMMARY

In summary, using  $(225.3 \pm 2.8) \times 10^6$   $J/\psi$  events collected with the BESIII detector, the decay of  $J/\psi \rightarrow \omega p\bar{p}$  in the decay mode  $\omega \rightarrow \gamma\pi^0$  is studied. The branching fraction  $\mathcal{B}(J/\psi \rightarrow \omega p\bar{p})$  is measured to be  $(9.0 \pm 0.2 (\text{stat.}) \pm 0.9 (\text{syst.})) \times 10^{-4}$ . No obvious enhancement around the  $p\bar{p}$  invariant-mass threshold is observed. At the 95% C.L., the upper limits on the product of branching fractions  $\mathcal{B}(J/\psi \rightarrow \omega X(p\bar{p}) \rightarrow \omega p\bar{p})$  are measured to be  $3.7 \times 10^{-6}$  and  $3.9 \times 10^{-6}$  with and without accounting for the Jülich FSI effect, respectively. As isospin for  $J/\psi \rightarrow \gamma p\bar{p}$  and  $\omega p\bar{p}$  should both favor  $I = 0$  ( $I = 1$  should be suppressed in  $J/\psi \rightarrow \gamma p\bar{p}$  as in other  $J/\psi$  radiative decays), the non-observation of  $X(p\bar{p})$  in  $\omega p\bar{p}$  disfavors the pure FSI interpretation for the  $p\bar{p}$  threshold enhancement in the decay  $J/\psi \rightarrow \gamma p\bar{p}$ .

## VI. ACKNOWLEDGMENT

The BESIII collaboration thanks the staff of BEPCII and the computing center for their hard efforts. This

work is supported in part by the Ministry of Science and Technology of China under Contract No. 2009CB825200; National Natural Science Foundation of China (NSFC) under Contracts Nos. 10625524, 10821063, 10825524, 10835001, 10935007, 11125525, 11235011; Joint Funds of the National Natural Science Foundation of China under Contracts Nos. 11079008, 11179007; the Chinese Academy of Sciences (CAS) Large-Scale Scientific Facility Program; CAS under Contracts Nos. KJCX2-YW-N29, KJCX2-YW-N45; 100 Talents Program of CAS; German Research Foundation DFG under Contract No. Collaborative Research Center CRC-1044; Istituto Nazionale di Fisica Nucleare, Italy; Ministry of Development of Turkey under Contract No. DPT2006K-120470; U. S. Department of Energy under Contracts Nos. DE-FG02-04ER41291, DE-FG02-05ER41374, DE-FG02-94ER40823; U.S. National Science Foundation; University of Groningen (RuG) and the Helmholtz Zentrum fuer Schwerionenforschung GmbH (GSI), Darmstadt; WCU Program of National Research Foundation of Korea under Contract No. R32-2008-000-10155-0.

- |  |  |
|--|--|
| <p>426 [1] J. Z. Bai <i>et al.</i> (BES Collaboration), Phys. Rev. Lett. <b>91</b>,<br/>427 022001 (2003).</p> <p>428 [2] M. Ablikim <i>et al.</i> (BES Collaboration), Chinese Physics<br/>429 <b>C 34</b>, 4 (2010).</p> <p>430 [3] M. Ablikim <i>et al.</i> (BES Collaboration), Phys. Rev. Lett.<br/>431 <b>108</b>, 112003 (2012).</p> <p>432 [4] J. P. Alexander <i>et al.</i> (CLEO Collaboration), Phys. Rev.<br/>433 <b>D 82</b>, 092001 (2010).</p> <p>434 [5] S. A. Athar <i>et al.</i> (CLEO Collaboration), Phys. Rev. <b>D</b><br/>435 <b>73</b>, 032001 (2006).</p> <p>436 [6] M. Ablikim <i>et al.</i> (BES Collaboration), Eur. Phys. J. <b>C</b><br/>437 <b>53</b>, 15 (2008).</p> | <p>438 [7] M. Ablikim <i>et al.</i> (BES Collaboration), Phys. Rev. Lett.<br/>439 <b>99</b>, 011802 (2007).</p> <p>440 [8] For review, S. Jin, Int. J. Mod. Phys. <b>A 20</b>, 5145 (2005).</p> <p>441 [9] A. Datta and P. J. O'Donnell, Phys. Lett. <b>B 567</b>, 273<br/>442 (2003).</p> <p>443 [10] M. L. Yan, S. Li, B. Wu, B. Q. Ma, Phys. Rev. <b>D 72</b>,<br/>444 034027 (2005).</p> <p>445 [11] S. L. Zhu, Int. J. Mod. Phys. <b>A 20</b>, 1548 (2005).</p> <p>446 [12] M. Abud, F. Buccella, F. Tramontano, Phys. Rev. <b>D 81</b>,<br/>447 074018 (2010).</p> <p>448 [13] B. S. Zou, H. C. Chiang, Phys. Rev. <b>D 69</b>, 034004 (2004).</p> |
|--|--|

- 449 [14] A. Sibirtsev, J. Haidenbauer, S. Krewald, U. Meissner, 471  
 450 A. W. Thomas, Phys. Rev. D **71**, 054010 (2005). 472
- 451 [15] D. V. Bugg, Phys. Lett. B **598**, 8 (2004). 473
- 452 [16] For review, C. S. Gao and S. L. Zhu, Commun. Theor. 474  
 453 Phys. **42**, 844 (2004); E. Klempt and A. Zaitsev, Phys. 475  
 454 Rept. **454**, 1 (2007). 476
- 455 [17] K. Abe *et al.* (BELLE Collaboration), Phys. Rev. Lett. 477  
 456 **94**, 182002 (2005). 478
- 457 [18] B. Aubert *et al.* (BABAR Collaboration), Phys. Rev. D 479  
 458 **74**, 051101 (2006). 480
- 459 [19] M. Ablikim *et al.* (BES Collaboration), Phys. Rev. Lett. 481  
 460 **95**, 262001 (2005); M. Ablikim *et al.* (BES Collabora- 482  
 461 tion), Phys. Rev. Lett. **106**, 072002 (2011). 483
- 462 [20] M. Ablikim *et al.* (BES Collaboration), Chinese Physics 484  
 463 C **36** (10), 915-928 (2012). 485
- 464 [21] M. Ablikim *et al.* (BES Collaboration), Nucl. Instrum. 486  
 465 Methods Phys. Res., Sect. A **614**, 345 (2010). 487
- 466 [22] J. Z. Bai *et al.* (BES Collaboration), Nucl. Instrum. 488  
 467 Methods Phys. Res., Sect. A **344**, 319 (1994); **458**, 489  
 468 627(2001). 490
- 469 [23] D. M. Asner *et al.* Int. J. Mod. Phys. A **24**, No. 1, 499 491  
 470 (2009).
- 471 [24] Z. Y. Deng *et al.* HEP & NP **30**, 371 (2006).
- 472 [25] S. Jadach, B. F. L. Ward and Z. Was, Comp. Phys. Com-  
 473 mu. **130**, 260 (2000); S. Jadach, B. F. L. Ward and Z.  
 474 Was, Phys. Rev. D **63**, 113009 (2001).
- 475 [26] R. G. Ping, Chin. Phys. C **32**, 599 (2008); D. J. Lange,  
 476 Nucl. Instrum. Meth. A **462**, 152 (2001).
- 477 [27] J. Beringer *et al.* (Particle Data Group), Phys. Rev. D  
 478 **86**, 010001 (2012).
- 479 [28] J. C. Chen, G. S. Huang, X. R. Qi, D. H. Zhang, Y. S.  
 480 Zhu, Phys. Rev. D **62**, 034003 (2000).
- 481 [29] W. D. Li, H. M. Liu *et al.* in proceeding of CHEP06,  
 482 Mumbai, India, 2006 edited by Sunanda Banerjee (Tata  
 483 Institute of Fundamental Research , Mumbai, 2006).
- 484 [30] W. Verkerke and D. Pirkby, eConf C0303241, MOLT007  
 485 (2003).
- 486 [31] M. Ablikim *et al.* (BES Collaboration), Phys. Rev. D **83**,  
 487 112005 (2011).
- 488 [32] M. Ablikim *et al.* (BES Collaboration), Phys. Rev. D **81**,  
 489 052005 (2010).
- 490 [33] M. Ablikim *et al.* (BES Collaboration), Phys. Rev. Lett.  
 491 **104**, 132002 (2010).